All-Optical Format Conversion-Based Flexible Optical Interconnection Using Nonlinear MZI With Nested-Pump Assisted NOLM

Qiankun Li, Xiongwei Yang, Huashun Wen, Qi Xu, Yameng Li, Jiali Yang, Huajun Yang, Heng Zhou, Pengfei Xu, Mark S. Leeson, *IEEE Senior Member,* Tianhua Xu, *IEEE Member*

Abstract—An all-optical format conversion (AOFC) scheme of star-m-ary quadrature amplitude modulation (star-mQAM) based on a nonlinear Mach-Zehnder interferometer (MZI) with nested-pump assisted nonlinear optical loop mirror (nested-PA-NOLM) is proposed and numerically simulated. In this scheme, input multi-Gbps star-8QAM signals can be converted into three quadrature phase shift keying (QPSK) signals (namely QPSK-A, -B and -C) through the PA-NOLM under different input power of the signal and the pump. The nonlinear MZI is formed by two PA-NOLMs of the upper and the lower arms, the former and the latter 3-dB optical couplers (OCs), a directional variable optical attenuator (VOA) in the upper arm and a directional variable phase shifter (VPS) in the lower arm. A VOA and a VPS are used to adjust the power ratio (PR) and relative phase shift (RPS) between any two of QPSK-A, -B and -C. When any two adjusted signals in QPSK-A, -B and -C are coherently superposed, the aggregated star-8QAM signal can be extracted again. Furthermore, the proposed scheme can also be used to convert the 20 Gbps bipolar 4-ary pulse amplitude modulation (PAM4) signal into two 10 Gbps BPSK signals and a 20 Gbps QPSK signal. When the proposed scheme is combined with the phase-sensitive amplification (PSA), it can also be used to convert one 16QAM into two QPSK signals. The scheme performance is analyzed via constellation diagrams, power waveforms, the error vector magnitude (EVM) and the bit error rate (BER) of the optical signals. The scheme can not only be deployed in optical gateways to connect optical networks using different modulation formats, but also has a potential applied advantage in security information transmission between different optical networks.

Index Terms—All-optical signal processing, quadrature amplitude modulation, self-phase modulation, cross-phase modulation, nonlinear optical loop mirror.

I. INTRODUCTION

WITH the development and application of the fifth-generation (5G) mobile communications, the Internet of Things (IoT), Internet of Energy (IoE), Ultra-high-definition (UHD) video flow, online working and other social software, various types of data traffic are being generated and processed in optical networks all the time. As Cisco predicted, nearly 300 billion mobile applications will be downloaded and some 5.3 billion Internet users are increasing at an annual compound growth rate (CAGR) of 6% by 2023 [1]. A large amount of data traffic generated will be transmitted between different optical networks through optical gateways. Therefore, the challenge of rapidly processing the continuously growing data traffic at optical gateways according to different optical network characteristics to realize all-optical interconnection of optical networks is of increasing importance. All-optical signal processing (AOSP) technologies can process optical signals at high transmission rates without the use of the optical-electrical-optical (O-E-O) conversion, which can relieve the signal processing pressure from optical gateways from increased data traffic [2]. In flexible all-optical networks (AONs), homogeneous and heterogeneous optical networks have been all-optical intra- and inter-connected via optical gateways, optical amplifiers and fiber components. Moreover, to improve the optical network performance, different optical signals with various modulation formats have also been explored to carry this data information. When optical signals have been transmitted in optical fiber links, optical amplifiers deployed at repeater nodes were used to extend optical signal transmission

distances. However, when the transmission of optical signals with different modulation formats between homogeneous and heterogeneous optical networks via connection nodes required all-optical format conversion (AOFC) operations be performed at optical gateways. Therefore, AOSP-based format conversion is an attractive optical gateway enabling technology for flexible optical interconnection of homogeneous and heterogeneous optical networks [3].

According to network size, service types, transmission distance, cost and other factors, different modulation formats have been used in different optical networks, such as long-haul backbone optical networks (BONs), middle-distance metro optical networks (MONs) and short-reach data centers (DCs). Intensity modulated signals can be received by direct detection (DD), which has the advantage of low cost and have thus become established in short-reach DCs, using, for example, on-off keying (OOK) and 4-ary pulse amplitude modulation (PAM4) [4-6]. Complex modulated signals offer higher spectrum efficiency (SE) and better chromatic dispersion (CD) tolerance, making them more suitable for long-haul optical transmission systems, implementing m-ary quadrature amplitude modulation (mQAM) and m-ary phase shift keying (mPSK). Therefore, AOFC between simple and advanced modulation formats, intensity modulation format, phase modulation format and quadrature amplitude modulation format can be used to realize all-optical interconnection of different optical networks. Moreover, many digital signal processing (DSP) methods can also be used to improve the optical signal transmission performance in coherent optical communication systems [2, 7, 8].

Since 8QAM signals have had a special applied advantage in wired and wireless optical transmission systems, the AOFC of several 8QAM signals have attracted much research attention [9-14]. Whether in fixed optical networks or in visible light communication (VLC) optical networks, the transmission performance of different 8QAM signals has also been investigated by simulations and experiments [15-21]. When the information flow was transmitted between heterogeneous optical networks, i.e., from fixed optical networks to VLC optical networks, the modulation formats of different 8QAM signals had to be interconverted at the optical gateway. The aggregation and de-aggregation between advanced and simple modulation formats were also one important function for all-optical networks (AONs) in realizing the all-optical interconnection of different optical networks. The aggregation and de-aggregation of OOK, QPSK and 8QAM had been proposed based on nonlinear effects in highly nonlinear fiber (HNLF) and semi-conductor optical amplifier (SOA) [13, 22, 23]. The aggregation and de-aggregation of BPSK and 8QAM have also been proposed based on nonlinear effects in HNLF [24, 25]. However, the SOA was an active device, which may increase the design complexity of the AOSP system. The de-aggregation devices from 8QAM to BPSK and QPSK were separated and designed based on nonlinear effects.

The star-8QAM signal can be seen as a QPSK signal with two-level intensity states. Compared to the other 8QAM signals,

it has the largest angular distance. Additionally, the better linewidth tolerance and easier implementation have also made it a promising modulation format [26]. This is especially the case for the coexistence of DSP-based passive optical networks (PONs) and 10-Gbps/λ OOK-based PONs, where the hierarchical characteristic of star-8QAM constellations have the applied advantage [27].
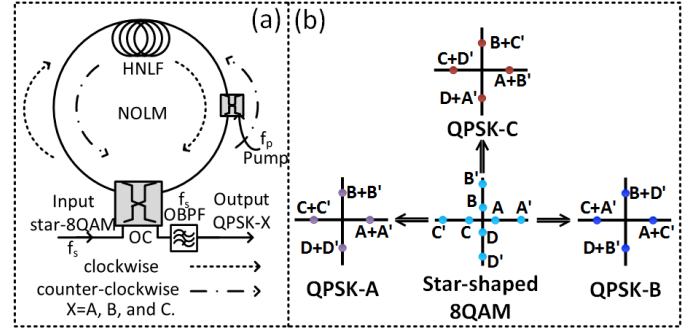
Fig. 1. Schematics of (a) the proposed pump-assisted NOLM and (b) constellations of star-8QAM to QPSK-A, QPSK-B and QPSK-C.
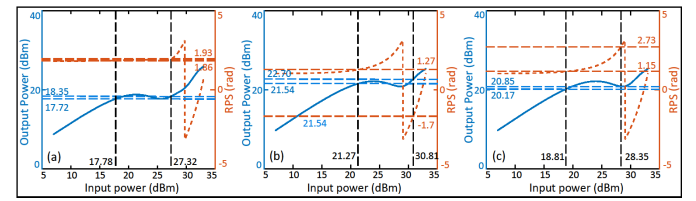
Fig. 2. PTF and RPS of all-optical format conversion from star-8QAM to (a) QPSK-A, (b) QPSK-B and (c) QPSK-C.

To the best of our knowledge, there has been no effective scheme to achieve all-optical aggregation and de-aggregation between star-8QAM and QPSK within a single format conversion device. In this paper, an AOFC scheme between star-8QAM and 3×QPSK based on a nonlinear Mach-Zehnder interferometer (MZI) with nested-pump assisted nonlinear optical loop mirror (nested-PA-NOLM) is proposed and numerically simulated. In the de-aggregation stage, the AOFC method PA-NOLM-based can be used to convert star-8QAM into three different types of QPSK (namely QPSK-A, -B and -C) only by changing the input power of the signal and the pump light. In the aggregation stage, by adjusting the power ratio (PR) and the relative phase shift (RPS) of any two types of QPSK-A, -B and -C, they can be aggregated into the star-8QAM signal (namely star-8QAM-AB, star-8QAM-AC and star-8QAM-BC) by coherent superposition. On one hand, this AOFC is beneficial to the all-optical interconnection of optical networks adopting star-8QAM and QPSK signals, respectively. On the other hand, it has a potential applied value in enhancing optical network security, e.g., implementing an all-optical logic XOR gate for format converted signals and improving the protection performance and fault tolerance with separated transmitted low-order signals [28, 29]. The constellation diagrams can be used to demonstrate the efficacy of the proposed AOFC scheme. The error vector magnitude (EVM) and the bit error rate (BER) of

the relative optical signals before and after the AOFC may be determined to evaluate the performance of the scheme. Furthermore, the proposed scheme can also achieve format conversion from 20 Gbps bipolar PAM4 signals to two 10 Gbps BPSK signals (namely BPSK-A and -B) and a 20 Gbps QPSK signal. Therefore, when the proposed scheme is mixed with phase-sensitive amplification (PSA), it can also de-aggregate a 10 Gbaud 16QAM signals into two 10 Gbaud QPSK signals.

II. THEORY AND OPERATING PRINCIPLE

A. De-aggregation from star-8QAM to three QPSK signals based on the tunable PA-NOLM

A schematic diagram of the PA-NOLM of converting star-8QAM into QPSK is shown in Fig. 1 (a). The input signal was divided into the clockwise (CW) signal and the counterclockwise (CCW) signal by a bi-directional 3-dB optical coupler (OC). The CCW signal was coupled with the CCW input pump light and they were sent into the HNLF. Meanwhile, the CW signal was also fed into the same HNLF. Therefore, the CW signal was only affected by the self-phase modulation (SPM) effect and the CCW signal will be affected by both SPM and the cross-phase modulation (XPM) introduced by the pump light. When the purely SPM phase-shifter CW signal was coherently mixed with the CCW signal, having both SPM and XPM phase shifts in the OC, the output signal could be filtered out by an optical band-pass filter (OBPF) with the same central frequency as the input. The nonlinear phase difference of the CW signal and the CCW signal could be used to change the amplitude and phase distributions of the output signal. For example, fig. 1 (b) shows constellations of converting input star-8QAM to three QPSK signals.

Based on the nonlinear Schrödinger equation, the output power transfer function (PTF) and the relative phase shift (RPS) of the output signal in the PA-NOLM can be expressed as [14]:

$$\begin{cases} P_{out} = M^2 + N^2 + 2MN\cos(\phi_M - \phi_N) \\ \phi_{rps} = \phi_{out} - \phi_{in} = \tan^{-1}\left[\dfrac{M\sin\phi_M + N\sin\phi_N}{M\cos\phi_M + N\cos\phi_N}\right] \end{cases} \quad (1)$$

where

$$\begin{cases} A^2 = P_0 J_1^2\left(2\gamma L\sqrt{P_0 P_1}\right) + P_1 J_0^2\left(2\gamma L\sqrt{P_0 P_1}\right) \\ M = \dfrac{\sqrt{P_{in}}}{2}; N = \dfrac{A}{\sqrt{2}} \\ \phi_N = \phi_{bom} + \dfrac{1}{4}\gamma L P_{in} + \dfrac{1}{2}\gamma L P_{pump} + \pi \\ \phi_{bom} = \tan^{-1}\left[\dfrac{\sqrt{P_0}J_1\left(2\gamma L\sqrt{P_0 P_1}\right)}{\sqrt{P_1}J_0\left(2\gamma L\sqrt{P_0 P_1}\right)}\right] \\ P_1 = \dfrac{1}{4}P_{in}; P_0 = \dfrac{1}{2}P_{pump}; \phi_M = \dfrac{1}{2}\gamma L P_{in} \end{cases} \quad (2)$$

P_{in} and P_{pump} are the input powers of the input and pump signals, respectively; P_{out} is the output signal power; ϕ_{in} and ϕ_{out} are the input and output phases, respectively, producing

the RPS ϕ_{rps}; γ and L are the nonlinear coefficient and the effective HNLF length, respectively.

The PTF and the RPS of the PA-NOLM used were applied to verify the format conversion from input star-8QAM to QPSK-A, -B and -C, respectively. The HNLF considered had a nonlinear coefficient of 13.1 (km·W)$^{-1}$, an effective length of ~550 m and a dispersion parameter of 1.6 ps (km·nm)$^{-1}$. The reference frequency was 193.1 THz and fiber losses were neglected.

When considering QPSK-A extracted from the input star-8QAM, the modulation index (MI) of the inner and the outer rings of the star-8QAM was 8/9. That meant the PR of the inner and the outer rings of the star-8QAM signal was 1/9. The input star-8QAM had a frequency of 193.1 THz with a 193.07 THz pump, at average powers of ~24.77 dBm (300 mW) and ~30.41 dBm (1100 mW), respectively. The PA-NOLM was designated PA-NOLM-A. The PTF and the RPS as functions of the power of the input optical signal were as shown in Fig. 2 (a). Since the powers of the inner and outer rings of the input star-8QAM were ~17.78 dBm (60 mW) and ~27.32 dBm (540 mW), respectively, the corresponding output powers were ~17.72 dBm and ~18.35 dBm. The corresponding RPS values of the inner and the outer rings were ~1.86 rad and ~1.93 rad, respectively. Although the output optical signal still had two intensity levels of the inner and the outer rings, the level interval was decreased from 9.54 dB to 0.63 dB. Thus, the level interval of 0.63 dB was negligible. The phase difference between the two corresponding RPSs was ~0.074 rad, i.e., ~4.25°. This means the inner ring and the outer ring constellations with the same phase of the input star-8QAM signal were converged together. The residual phase difference of just 4.25° was deemed acceptable since it was much less than the input star-8QAM signal 45° phase difference. Namely, the input star-8QAM signal had been converted into QPSK-A, as shown in Fig. 1 (b).

When considering the format conversion from input star-8QAM to QPSK-B with the same HNLF, the PTF and the RPS functions with the input power were also verified, as shown in Fig. 2 (b). The PA-NOLM was here designated PA-NOLM-B. The input signal was a ~28.26 dBm (average power: 670 mW) star-8QAM signal and the input pump power was ~29.54 dBm (average power: 900 mW). Since the input inner and outer rings of the star-8QAM signal had powers of ~21.27 dBm (average power: 134 mW) and ~30.81 dBm (average power: 1206 mW), respectively, the corresponding output powers were 21.54 dBm and 22.70 dBm. The power gap between the output inner and outer rings decreased from 9.54 dB to 1.16 dB. For the input star-8QAM, the corresponding output RPSs of the inner and the outer rings were ~1.27 rad and ~-1.7 rad, respectively. Thus, there is a phase difference gap of ~169.7°, which is again close to 180°. Considering the nonlinear phase shift induced by SPM, the outer ring constellations of input star-8QAM will obtain a bigger SPM phase shift than the inner ring constellations of that. Therefore, the power gap of 1.16 dB and the phase difference error of ~10.3° could be ignored. This also means the inner ring

and the outer ring constellations with antiphase converged together. Namely, QPSK-B can be obtained from input star-8QAM, as shown in Fig.1 (b).

For star-8QAM to QPSK-C conversion with the same HNLF, the PTF and the RPS with the input signal power were determined and are shown in Fig. 2 (c) using a ~29.54 dBm (average power: 900 mW) pump. The PA-NOLM was here designated PA-NOLM-C. When the input signal had an average power of ~25.80 dBm (380 mW), the corresponding inner and outer ring powers were ~18.81 dBm (average power: 76 mW) and ~28.35 dBm (average power: 684 mW), respectively. The corresponding output powers were ~20.17 dBm and ~20.85 dBm, respectively. The power gap decreased from 9.54 dB to 0.68 dB. Thus, the amplitude error was negligible. Moreover, for the input star-8QAM signal, the corresponding RPS values of the inner and the outer rings were ~1.15 rad and ~2.73 rad, respectively, i.e., a gap of ~1.58 rad or ~90.4°. Compared to the inherent angular phase of 90°, the ~0.40° phase error was negligible. This means that the inner ring and the outer ring constellations of input star-8QAM with an angular phase of 90-degree were merged together. Namely, conversion from the input star-8QAM signal to QPSK-C could be achieved, as shown in Fig. 1 (b).

Therefore, the de-aggregation configuration from input star-8QAM to QPSK-A, -B and -C can be equipped with an optical gateway to connect optical networks with different modulation formats. For example, in a point-to-multi-point (P2MP) optical network, the de-aggregation from star-8QAM to three QPSK signals can be used to realize the de-aggregation of data traffic from a BON to local access networks (LANs). Moreover, all converted QPSK-A, -B or -C, can be obtained from the same format conversion device by changes to the signal and pump power levels.

B. Aggregation from any two QPSK signals of QPSK-A, -B and -C to the star-8QAM signal based on coherent addition

In an 8QAM signal, each symbol represents three bits whereas in QPSK it is only two bits. In the de-aggregation stage, the bit information of the input star-8QAM signal was transferred into three QPSK signals. Any two of these could be aggregated through coherent addition [30]. When this is implemented, as shown in Fig. 3, the aggregated star-8QAM signal has the same data information as the input star-8QAM signal, maintaining information integrity. This can also be seen some of the star-8QAM signal's information bits being concealed in the converted QPSK signals, which can be transmitted separately by different optical transmission links. To ensure the bit information integrity of the star-8QAM signal, the separated QPSK signals must be combined by coherent addition at the destination. Possession of any two converted QPSK signals enables a receiver to restore the original bit information. Moreover, the separated transmission of the de-aggregated QPSK signals offers assistance to secure optical communication [29] since if an attacker (Eve) was in possession of just one converted QPSK signal, it would be very difficult to recover the original star-8QAM information. For the separated

transmitted QPSK signals, it will be extremely difficult for an Eve to simultaneously acquire two separated QPSK signals in a real optical transmission link. The aggregated star-8QAM signal can be recovered by authorized receivers via the coherent addition of two QPSK signals. By adjusting the PR and RPS of any two types of QPSK-A, -B and -C, the optical field of the coherent superposed optical signal can be expressed as:

$$E_{agg-star-8qam} = A_{qpsk-x}e^{i\phi_{qpsk-x}}10^{-\frac{\alpha}{20}}$$
$$+A_{qpsk-y}e^{i\phi_{qpsk-y}}e^{i\Delta\phi} \qquad (3)$$

α and $\Delta\phi$ represent the power attenuation coefficient of QPSK-X and the linear phase shift of QPSK-Y with $x \neq y$ ($x, y = A, B$ or C).

In the progress of coherent addition of two of QPSK-A, -B and -C to form the aggregated star-8QAM signal, an issue should be mentioned in the practical experiment. Since two of QPSK-A, -B and -C were transmitted by different optical links, the slowly varying relative phase difference caused by passing through different fiber paths may result in temporal phase and amplitude fluctuation. Each of the fiber path had different characteristics, vibration, temperature fluctuation, and so on. Therefore, some active and passive phase stability methods should be considered in the practical experiment to eliminate the instability brought by temperature fluctuation, airflow, vibration, curvature, splitting ratio and so on [31-35].
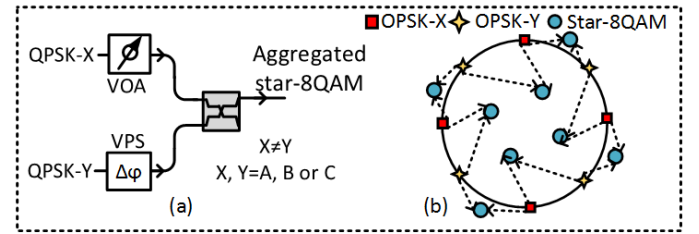
Fig. 3. Aggregation (a) configuration and (b) constellations from two QPSK to star-8QAM signals.
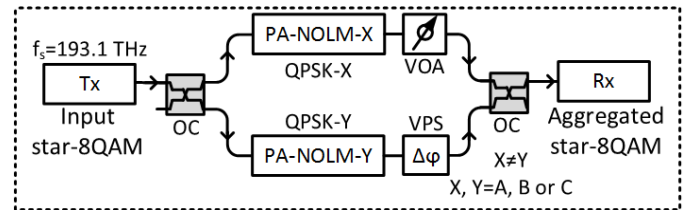
Fig. 4. The proposed aggregation and de-aggregation scheme for the star-8QAM signal, Tx: Transmitter, Rx: Receiver.

III. SIMULATIONS AND DISCUSSIONS

The proposed AOFC scheme based on the nonlinear MZI with nested-PA-NOLM is shown in Fig. 4. In the numerical simulation, a 10 Gbaud star-shaped 8QAM signal at a central frequency of 193.1 THz could be generated by a cascade phase modulator (PM) and amplitude modulator (AM) driven by the pseudo-random binary sequence (PRBS). In the transmitter, the input non-return-to-zero (NRZ) pulse has the rise time of 2.5×10^{-11} s. The linewidth of the continuous wave (CW) laser

was neglected. An amplified spontaneous emission (ASE) noise source was used to change the input optical signal-to-noise ratio (OSNR) followed by an optical band-pass filter (OBPF) to remove the out-of-band noise. The generated star-8QAM signal was launched into the nonlinear MZI with nested-PA-NOLM, which was formed by two 3-dB OCs and two PA-NOLMs. The former OC was used to separate the input star-8QAM signal into the upper arm and the lower arm optical signals. For the de-aggregation processing, a 193.07 THz pump light was coupled into the PA-NOLM. The latter OC was used to converge the upper arm and the lower arm converted QPSK signals into the star-8QAM signal. As analyzed in Section II.A, the fiber used in the PA-NOLM had a nonlinear coefficient of 13.1 $(km \cdot W)^{-1}$, an effective length of ~550 m and a dispersion parameter of 1.6 ps $(km \cdot nm)^{-1}$; the reference frequency was 193.1 THz and fiber losses were neglected. Using a ~24.77 dBm input star-8QAM signal and ~30.41 dBm pump enabled the converted QPSK-A to be obtained. Similarly, using corresponding powers of ~28.26 dBm and ~29.54 dBm, respectively produced QPSK-B and ~25.80 dBm and ~29.54 dBm delivered QPSK-C. The constellations from star-8QAM to QPSK-A, -B and -C with an input OSNR of 27 dB are shown in Fig. 5.
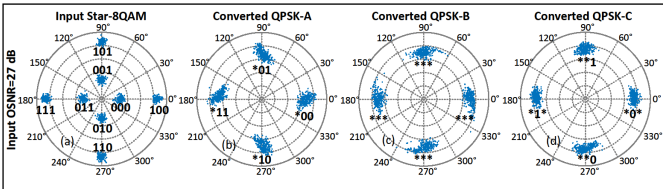

Fig. 5. Constellations of (a) the input star-8QAM and converted (b) QPSK-A, (c) QPSK-B and (d) QPSK-C, * means hidden bit (0 or 1 depending on the case) in Fig. 1 (b).
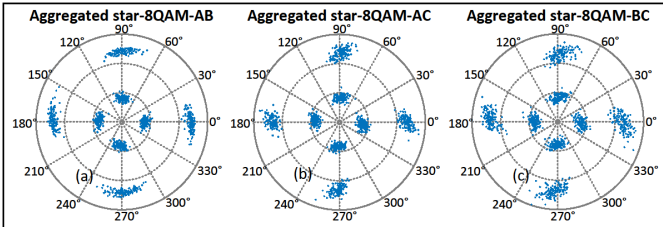

Fig. 6. Constellations of the aggregated star-8QAM signals.

For the aggregation processing, when considering QPSK-A and QPSK-B combined to obtain the star-8QAM signal, the VOA and the VPS were 3 dB and -36°, respectively. The average powers of QPSK-A and QPSK-B were ~14.62 dBm and ~20.45 dBm, respectively. The constellations of the aggregated star-8QAM signal (namely star-8QAM-AB) are shown in Fig. 6 (a). When the VOA and the VPS were 1.8 dB and -62°, respectively, QPSK-A (average power: ~15.81 dBm) and QPSK-C (average power: ~19.24 dBm) could be coherently superposed into the star-8QAM signal (namely star-8QAM-AC), as shown in Fig.6 (b). When the VOA and the VPS were set to be 3.6 dB and -27°, respectively, QPSK-B (average power: ~16.9 dBm) and QPSK-C (average power: ~19.24 dBm) were

aggregated into the star-8QAM signal (namely star-8QAM-BC), as shown in Fig. 6 (c).

To compare the bit sequence variance of the 8QAM signal before and after de-aggregation and aggregation, the power waveforms of the input star-8QAM signal and the aggregated star-8QAM-AB, -AC and -BC were also measured, as shown in Fig. 7. Clearly, the aggregated star-8QAM-AB, -AC and -BC had the same bit sequence as the input star-8QAM signal. This phenomenon indicated that the original bit information of the input star-8QAM signal can be restored from the coherent addition of any two converted QPSK signals. Moreover, from the constellations of the aggregated star-8QAM-AB signal, the amplitude noise of the outer ring was regenerated compared to the input star-8QAM signal. This can also be identified from the power waveform of the aggregated star-8QAM-AB signal, as shown in Fig. 7 (b). In addition to information integrity, the bit mapping of optical signals before and after format conversion was another key question. From the format conversion rules introduced in Section II, for an input star-8QAM signal with Gray coding, the converted QPSK-A obtained the phase information of the star-8QAM signal. The intensity information of the inner and the outer rings of the star-8QAM signal had been hidden into the phase states of the converted QPSK-B and QPSK-C. This can also be seen as information hiding or encryption of intensity information. Only by coherently stacking two converted QPSK signals with specific logical relationships could the intensity information of the original star-8QAM signal be restored.
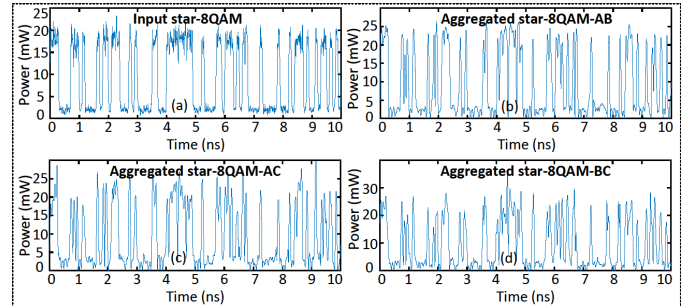
Fig. 7. Power waveforms of (a) the input star-8QAM signal with an input OSNR of 27 dB, (b) the aggregated star-8QAM-AB signal, (c) the aggregated star-8QAM-AC signal and (d) the aggregated star-8QAM-BC signal.

The bit allocation on each of the constellation point of star-8QAM constellation and that for the converted QPSK-A, -B, and -C were also described to make sure that the original bit information on the star-8QAM was correctly transferred to the converted QPSK signal. For example, the bit allocation of the inner star-8QAM constellation was 000, 001, 011, 010 on 0°, 90°, 180°, 270°, and the outer constellation was 100, 101, 111, 110 on 0°, 90°, 180°, 270°, respectively, as a Gray code was considered, as shown in Fig. 8. In this case, the bit allocation of QPSK-A was *00, *01, *11, *10 on 0°, 90°, 180°, 270° where * means hidden bit (0 or 1 depending on the case) in Fig. 1(b). Thus, only two bit information was transferred to QPSK-A. The

bit allocation of QPSK-B was ***, ***, ***, *** on 0°, 90°, 180°, 270°, resulted in no bit transfer. The bit allocation of QPSK-C was *0*, **1, *1*, **0 on 0°, 90°, 180°, 270°, resulted in one bit transfer. Therefore, the original bit information on the star-8QAM cannot be obtained especially by QPSK-B. Only when any two of QPSK-A, -B and -C are coherently combined, the original bit information of the input star-8QAM signal could be reshaped.

Fig. 8. (a) EVM versus input OSNR, (b) BER versus receiver OSNR for de-aggregation from input star-8QAM to QPSK-A, -B and -C with the input OSNR of 27 dB.

Fig. 9. (a) EVM versus input OSNR, (b) BER versus receiver OSNR for aggregation from any two QPSK signals to the aggregated star-8QAM signal at an input OSNR of 27 dB.

The EVM variance with the input OSNR and the BER variance with the receiver OSNR were used to evaluate the AOFC scheme performance. It is worth noting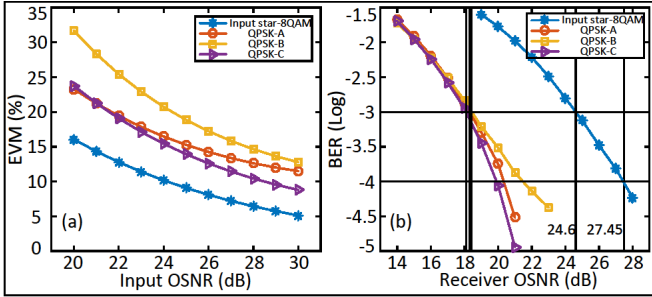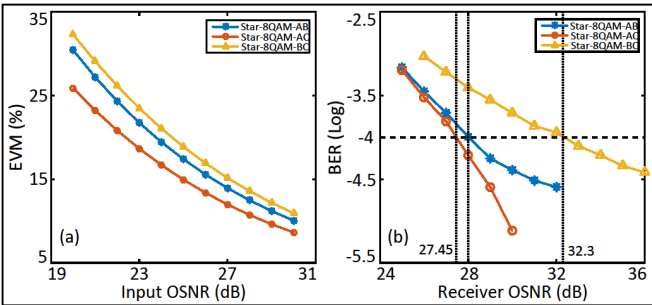 that there is no using some DSP technique in calculating the BER performance. Fig. 8 shows the EVM and BER performance of the optical signals for the de-aggregation processing from input star-8QAM to QPSK-A, -B and -C. As seen in Fig. 8 (a), with improving input OSNR, the three converted QPSK signals had worse EVM performance than the input star-8QAM. This was due to the accumulation of nonlinear phase noise and amplitude noise generated by the PA-NOLM. When the input OSNR of star-8QAM was 27 dB, the corresponding EVMs of star-8QAM, QPSK-A, -B and -C were ~7.22%, ~13.37%, ~15.84% and ~11.44%, respectively. However, the three converted QPSK signals exhibited better BER performance than the input star-8QAM signal with improving receiver OSNR, as shown in Fig. 8 (b). With a BER threshold of 10^{-3}, the corresponding receiver OSNRs for star-8QAM, QPSK-A, -B and -C were ~24.6 dB, ~18.3 dB, ~18.4 dB and ~18.1 dB, respectively. Thus, the converted signals displayed an improvement in receiver OSNR of at least 6.3 dB over the input star-8QAM. This is not unexpected since QPSK had a larger Euclidean distance

between adjacent constellations than the jointly amplitude and phase modulated star-8QAM signal. The smallest Euclidean distance of star-8QAM was strongly dependent on the PR of star-8QAM between the inner and the outer rings. For input star-8QAM with a PR of 1/9, the inner ring constellations were more distorted by amplitude and the phase noise.

For the aggregation processing from any two QPSK signals to the aggregated star-8QAM signal, the EVM and the BER performance were also determined, as shown in Fig. 9. When the input OSNR was set to be 27 dB, the corresponding EVMs of the aggregated star-8QAM-AB, -AC and -BC were ~13.93%, ~11.97% and ~15.15%, respectively, as shown in Fig. 9 (a). The aggregated star-8QAM-BC had the worst EVM performance, and the aggregated star-8QAM-AC the best. As for the BER performance of the three aggregated star-8QAM-AB, -AC and -BC, using a BER threshold of 10^{-4}, the corresponding receiver OSNRs were ~28 dB, ~27.45 dB and ~32.3 dB, respectively, as shown in Fig. 9 (b). Compared to the aggregated star-8QAM-BC signal, the aggregated star-8QAM-AB and star-8QAM-AC had 4.3 dB and 4.85 dB performance improvement in receiver OSNR, respectively. As shown in Fig. 8 (b), at a BER threshold of 10^{-4}, the corresponding receiver OSNR for the input star-8QAM signal was ~27.45 dB. Therefore, although the aggregated star-8QAM-AC had worse EVM performance than the input star-8QAM signal, it offered similar BER performance to the input star-8QAM signal. This was mainly because the anti-noise ability of the 8QAM signal was not relevant to the amplitude and the phase noise in constellations. However, the Euclidean distance between the adjacent constellations did play a significant part, for example, the phase distance (PD) between inner ring adjacent constellations and the amplitude distance (AD) between adjacent inner and outer ring constellations with the same phase states [13]. The aggregated star-8QAM-AB and star-8QAM-BC signals also had about 4.3 dB and 4.85 dB performance degradation in receiver OSNR compared to the input star-8QAM signal, respectively. The OSNR penalty was primarily caused by the extra amplitude and phase noise brought by the SPM, XPM effects and coherent addition in the PA-NOLM.

We also considered 10 Gbaud bipolar PAM4, which can be seen as the simplest star-QAM signal. It can be generated through the coherent addition of two BPSK signals [36, 37] and has attracted considerable research attention since it can be received by coherent or direct detection [38-40]. Recently, there have also been improvements in bipolar PAM4 format conversion schemes [41, 42]. However, these produced two de-aggregated BPSK signals with different wavelengths, which may lead to decreased wavelength utilization. Format conversion from bipolar PAM4 to QPSK has also been performed based on SPM and power saturation in a SOA [43]. This increased the scheme complexity since it employed an active device rather than a HNLF. Although another format conversion scheme from bipolar PAM4 to QPSK was proposed based on SPM in a single HNLF, the converted QPSK was not uniform in amplitude [44]. Here, the PA-NOLM scheme enables the conversion of an input bipolar PAM4 signal into BPSK-A, -B and QPSK signals for different input signals and pump powers. The constellations of the input bipolar PAM4 signal before and after format conversion are shown in Fig. 10.

The PR of the inner and the outer rings for the input bipolar PAM4 signal was also 1/9. As analyzed above, when the input bipolar PAM4 signal and pump had average powers of ~24.77 dBm and ~30.41 dBm, respectively, BPSK-A results. Using average powers of ~28.26 dBm and ~29.54 dBm for the input bipolar PAM4 signal and pump, respectively delivers BPSK-B. Finally, for the input bipolar PAM4 signal and pump average powers of ~25.80 dBm and ~29.54 dBm, respectively, QPSK can be received. It was noteworthy that the converted BPSK-A and -B could be seen as the de-aggregation of the input bipolar PAM4 signal. For the format conversion from bipolar PAM4 to QPSK, the intensity information of bipolar PAM4 was transferred into the phase information of QPSK.
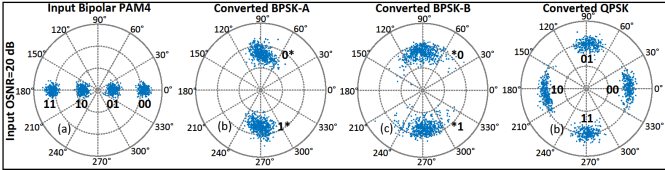

Fig. 10. Constellations of (a) the input 20 Gbps bipolar PAM4 signal, (b) the converted BPSK-A signal, (c) the converted BPSK-B signal and (d) the converted QPSK signal.

One bit allocation case could be considered for the input bipolar PAM4 signal, e. g., the inner constellation was 01 and 10 on 0° and 180°, and the outer constellation was 00 and 11 on 0° and 180°, respectively, as shown in Fig. 10 (a). The converted BPSK-A and BPSK-B signals can obtain the first and second bit information of the input bipolar PAM4 signal, respectively, as shown in Fig. 10 (b)-(c). The converted QPSK signal could obtain all the bit information of the input bipolar PAM4 signal, as shown in Fig. 10 (d). Therefore, the information integrity of the input bipolar PAM4 signal can be preserved before and after AOFC. In addition, the two converted BPSK-A and BPSK-B can also be aggregated into the bipolar PAM4 and the QPSK signals again through coherent addition.
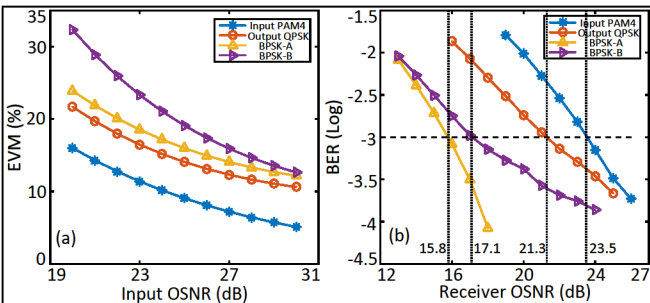

Fig. 11. (a) EVM versus input OSNR, (b) BER versus receiver OSNR for conversion of bipolar PAM4 to BPSK-A, -B and QPSK at an input OSNR of 20 dB.

The EVM and BER performance of the input bipolar PAM4 signal before and after AOFC were determined, as shown in Fig. 11. When the input bipolar PAM4 signal had an input OSNR of 20 dB, the EVMs of the bipolar PAM4 signal, the converted BPSK-A, BPSK-B and QPSK signals are ~16.01%, ~23.88%, ~32.34% and ~21.68%, respectively, as shown in Fig. 11 (a).

The converted BPSK and QPSK signals had demonstrably worse EVM performance than the input bipolar PAM4 signal because of the extra amplitude and phase noise generated by the PA-NOLM. However, better BER performance for the converted BPSK and QPSK signals can be obtained compared to the input bipolar PAM4 signal with an input OSNR of 20 dB, as shown in Fig. 11 (b). Using a 10^{-3} BER threshold, the corresponding receiver OSNRs of the input bipolar PAM4 signal, the converted BPSK-A, BPSK-B and QPSK signals were ~23.5 dB, ~15.8 dB, ~17.1 dB and ~21.3 dB, respectively. Thus, the converted BPSK-A, BPSK-B and QPSK signals can offer 7.7 dB, 6.4 dB and 2.2 dB improvements in receiver OSNR, respectively. The BPSK signal as the lowest-order phase modulated signal had the largest Euclidean distance between the adjacent constellations. This made the BPSK signal usually have better BER performance than the other high-order modulated signals. The all-optical de-aggregation from bipolar PAM4 to BPSK signals can be used in the scenario of P2MP. Additionally, in the presence of extremely noisy links, unsuitable for direct transmission of bipolar PAM4, the de-aggregated BPSK signals could be used to transmit the data information separately. A simple combination operation between the two separated BPSK signals could be used to ensure the information integrity.

For the converted QPSK signal, the Euclidean distance in phase states between the adjacent constellations delivered better anti-noise ability. Although the converted QPSK signal was affected by the generated extra phase noise, it also had better BER performance than the input bipolar PAM4 signal. Moreover, existing AOFC schemes from bipolar PAM4 to QPSK have been realized based on PSA, SPM and SOA or HNLF power saturation effects [43-45]. Our scheme avoids the phase-locking operations of PSA, obtains a uniform amplitude distribution for the converted QPSK signal and improves its anti-noise ability.

In addition, the AOFC of 16QAM was also considered due to its potential application in high-speed and large-capacity optical networks [46-48]. On one hand, the 16QAM can be de-aggregated into two quadrature bipolar PAM4 signals or two QPSK signals by nonlinear optical signal processing [43, 44, 49, 50]. On the other hand, the 16QAM can also be produced by the coherent addition of two bipolar PAM4 signals or two QPSK signals by linear and nonlinear optical signal processing [36, 37, 51, 52]. Modulation format aggregation from simple to complex modulation formats may assist data traffic aggregation from different users to the same destination, i.e., multi-point-to-point (MP2P) optical transmission. Conversely, de-aggregation from the complex to simple modulation formats has utility in realizing data grooming, and simplifying receivers and optical switching by adding/dropping the sub-optical signal. The development of optical constellation slicing (OCS) and constellation add/drop multiplexers (CADMs), have brought complex to simple de-aggregation technology to reality [53, 54]. Utilization of PSA for de-aggregating a 16QAM signal into two bipolar PAM4 signals (PAM4-I and PAM4-Q) has also been investigated numerically and experimentally [44, 50]. However, QPSK finds more application in long-haul transmission than PAM4 [55] making de-aggregation from 16QAM to 2×QPSK the research hot spot. Here, we thus investigated an all-optical

constellations de-multiplexing scheme from 10 Gbaud 16QAM to 2×QPSK by combining PSA and the PA-NOLM, as shown in Fig. 12. The input 16QAM was firstly de-aggregated into two bipolar PAM4 signals by the dual-pump degenerate PSA. Two pumps, both with average power ~18.45 dBm (f_{p1}=193.07 THz and f_{p2}=193.13 THz), and the input 16QAM signal with average power ~6.99 dBm (f_s=193.1 THz) were injected into a HNLF to obtain PAM4-I and PAM4-Q by phase-sensitive compression of the input signal constellations. The PSA gain axis could be adjusted by adding a linear phase shift to the input signal and pump lights. After adjusting the bipolar PAM4 signal and the pump powers to 24.77 dBm and 29.19 dBm, respectively, the bipolar PAM4 signal was injected into the PA-NOLM to generate the converted QPSK signal, as shown in Fig. 13.
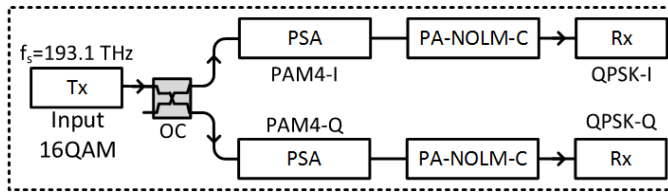

Fig. 12. Schematic diagram of the de-aggregation from 16QAM to 2×QPSK based on PSA and PA-NOLM.
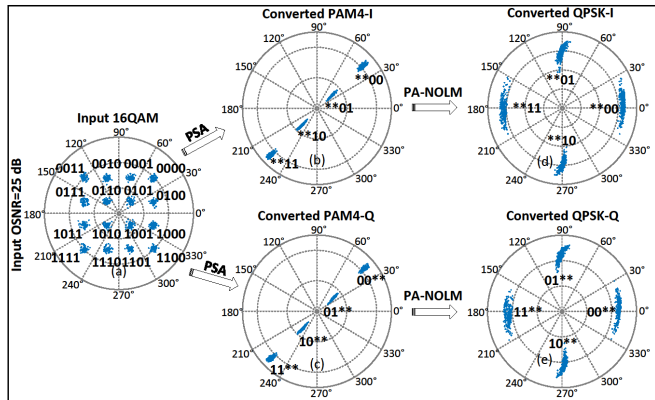

Fig. 13. Constellations of (a) the input 40 Gbps 16QAM signal, (b) the converted PAM4-I signal, (c) the converted PAM4-Q signal, (d) the converted QPSK-I signal and (e) the converted QPSK-Q signal.

One bit allocation case could also be considered for the input 16QAM signal, as shown in Fig. 13 (a). The last two and the first two bit information of the input 16QAM signal can be transferred into the intermediate converted PAM4-I and PAM4-Q signals, respectively, as shown in Fig. 13 (b)-(c). Then, the final converted QPSK-I and QPSK-Q signals can obtain the last two and the first two bit information of the input 16QAM signal, respectively, as shown in Fig. 13 (d)-(e). As such, the information integrity of the input 16QAM signal can also be preserved before and after AOFC. In addition, the two converted QPSK-I and QPSK-Q signals can also be aggregated into the square- and star-16QAM signals through coherent addition.

Compared to present 16QAM to 2×QPSK de-aggregation schemes [43, 44, 49, 54], the proposed scheme has some advantages: 1) It does not require an active device, such as a SOA. 2) The converted QPSK maintains the same wavelength as the input 16QAM signal. 3) No high-order harmonics are needed to generate the phase-locked pump light by injection locking (IL). 4) The converted QPSK has a more uniform amplitude state, which is also beneficial to further de-aggregate the QPSK into two BPSK signals based on PSA. 5) Any converted QPSK signal can also be added or dropped and coherently added with the new input QPSK signal to generate the new 16QAM signal. This characteristic may be useful to construct a flexible optical network based on CADM.
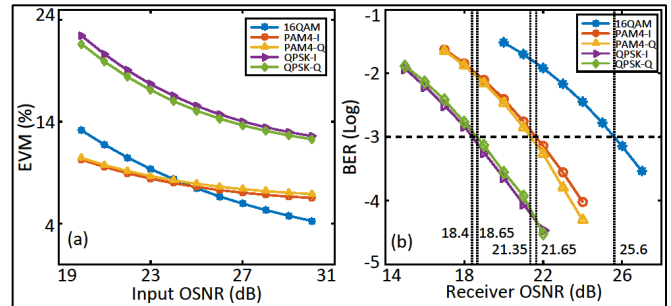

Fig. 14. (a) EVM versus input OSNR, (b) BER versus receiver OSNR for conversion of 16QAM to 2×QPSK at an input OSNR of 25 dB.

The EVM and the BER performance of the 16QAM signal before and after format conversion were calculated, as shown in Fig. 14. For the input 16QAM signal with an input OSNR of 25 dB, the corresponding EVMs of the 16QAM signal, the converted PAM4-I and PAM4-Q, the converted QPSK-I and QPSK-Q signals were ~7.47%, ~7.60%, ~7.91%, ~15.56% and ~15.09%, respectively, as shown in Fig. 14 (a). With the improvement of the input OSNR, the EVM performance of the converted QPSK-I and -Q signals became worse than the input 16QAM signal. When the input OSNR was larger than 25 dB, the EVM performance of the converted PAM4-I and -Q was worse than the input 16QAM signal. When the input OSNR was smaller than 25 dB, the converted PAM4-I and -Q signals had better EVM performance than the input 16QAM signal. This meant that for greater OSNR, the conversion of phase noise to amplitude noise based on PSA formed the main source of the degradation of the EVM performance. The converted bipolar PAM4 signals (PAM4-I and PAM4-Q) were mainly affected by amplitude noise.

As shown in Fig. 14 (b), for a BER threshold of 10^{-3}, the corresponding receiver OSNRs for the input 16QAM signal with an input OSNR of 25 dB, the converted PAM4-I and -Q, the converted QPSK-I and -Q were ~25.6 dB, ~21.65 dB, ~21.35 dB, ~18.4 dB and ~18.65 dB, respectively. Therefore, the converted bipolar PAM4 and QPSK signals offered greater noise immunity than the input 16QAM signal. For example, the converted PAM4-I signal had an approximately 3.95 dB improvement in receiver OSNR, whilst the corresponding improvement was around 7.2 dB for the converted QPSK-I signal. Additionally, compared to the PAM4-I signal as one amplitude and phase joint modulated signal, the QPSK-I signal as one phase modulated signal had about 3.25 dB performance improvement in the receiver OSNR. Notably, for the converted

QPSK signals, the constellations lying in the quadrature axis, which were converted by the inner ring constellations of the bipolar PAM4 signals, were mainly affected by amplitude noise. The constellations lying in the in-phase axis, which were converted by the outer ring constellations of the bipolar PAM4 signals, had larger phase noise. To some extent, the non-uniform distribution of amplitude and phase noise can also be seen as the phase regeneration for the constellations in the quadrature axis and the amplitude regeneration for the constellations in the in-phase axis.

IV. CONCLUSION

In this paper, an all-optical constellations aggregation and de-aggregation scheme from star-8QAM to 3×QPSK using nonlinear MZI with nested-PA-NOLM has been proposed and numerically simulated. When the input OSNR was set to 27 dB, the constellation and eye diagrams were assessed to intuitively evaluate the star-8QAM signal format conversion results. For the de-aggregation from input star-8QAM to 3×QPSK, there was at least ~6.3 dB improvement in the receiver OSNR for the three converted QPSK signals. For the aggregated 3×star-8QAM, the BER performance of the aggregated star-8QAM-BC was worse than the other two aggregated star-8QAM-AB and -AC. Meanwhile, the proposed scheme could achieve the all-optical de-aggregation from input bipolar PAM4 to 2×BPSK and the format conversion from input bipolar PAM4 to QPSK. Both the converted BPSK signals and the converted QPSK signal both achieved better anti-noise performance. Moreover, when the proposed scheme was combined with PSA technology, the input 16QAM could also be de-aggregated into 2×QPSK. Moreover, compared to the input 16QAM signal with an input OSNR of 25 dB, the converted QPSK signal obtained at least 7.2 dB BER performance improvement. The scheme can not only be deployed in optical gateways to connect optical networks using different modulation formats, but also has a potential applied advantage in security information transmission between different optical networks.

REFERENCES

[1] Cisco Annual Internet Report (2018-2023) White Paper (2020), https://www.cisco.com/c/en/us/solutions/collateral/executive-perspectives/annual-internet-report/white-paper-c11-741490.html.

[2] A. E. Willner, A. Fallahpour, F. Alishahi, Y. Cao, A. Mohajerin-Ariaei, A. Almaiman, P. Liao, K. Zou, A. N. Willner, and M. Tur, "All-Optical Signal Processing Techniques for Flexible Networks," J. Lightwave Technol., vol. 37, no. 1, pp. 21-35, 2019.

[3] K. Mishina, D. Hisano and A. Maruta, "All-optical modulation format conversion and applications in future photonic networks", IEICE Trans. Electron., vol. 102, pp. 304-315, 2019.

[4] Haik Mardoyan, Miquel A. Mestre, Jose Manuel Estarán, Filipe Jorge, Fabrice Blache, Philippe Angelini, Agnieszka Konczykowska, Muriel Riet, Virginie Nodjiadjim, Jean-Yves Dupuy, and Sebastien Bigo, "84-, 100-, and 107-GBd PAM-4 Intensity-Modulation Direct-Detection Transceiver for Datacenter Interconnects," J. Lightwave Technol. 35, 1253-1259 (2017).

[5] José Manuel Estarán, Haik Mardoyan, Filipe Jorge, Oskars Ozolins, Aleksejs Udalcovs, Agnieszka Konczykowska, Muriel Riet, Bernadette Duval, Virginie Nodjiadjim, Jean-Yves Dupuy, Xiaodan Pang, Urban Westergren, Jiajia Chen, Sergei Popov, and Sébastien Bigo, "140/180/204-Gbaud OOK Transceiver for Inter- and Intra-Data Center Connectivity," J. Lightwave Technol. 37, 178-187 (2019).

[6] Mingzhu Yin, Xiaowu Wang, Dongdong Zou, Wei Wang, Qi Sui, and Fan Li, "Low cost O-band inter-datacenter interconnect utilizing a 4-bit resolution digital-to-analog converter for PAM-4 signal generation," Opt. Express 29, 31527-31536 (2021).

[7] K. Kikuchi, "Fundamentals of Coherent Optical Fiber Communications," in Journal of Lightwave Technology, vol. 34, no. 1, pp. 157-179, 1 Jan.1, 2016.

[8] J. Zhao, Y. Liu, and T. Xu, "Advanced DSP for Coherent Optical Fiber Communication," Appl. Sci. 9(19), 4192 (2019).

[9] B. Zhang et al., "An all-optical modulation format conversion for 8QAM based on FWM in HNLF", IEEE Photon. Technol. Lett., vol. 25, no. 4, pp. 327-330, Feb. 2013.

[10] H. Liu, H. Wang, and Y. Ji, "Simultaneous All-Optical Channel Aggregation and De-Aggregation for 8QAM Signal in Elastic Optical Networking," IEEE Photonics Journal, vol. 11, no. 1, pp. 1-8, 2019.

[11] F. Wan, B.-J. Wu, F. Wen and K. Qiu, "All-optical modulation format conversion from star-QAM to PSK and ASK signals", Opt. Commun., vol. 451, pp. 23-27, Nov. 2019.

[12] Q. Li, J. Yang, X. Yang, Q. Xu, H. Zhang, Y. Liang, and H. Yang, "All-Optical Format Conversion of 2-Dimensional MQAM to MPSK Based on Nonlinear Mach-Zehnder Interferometer with Wavelength Preservation," J. Lightwave Technol., vol. 40, no. 22, pp. 7246-7253, 2022.

[13] Q. Li, X. Yang, H. Wen, Q. Xu, J. Yang, and H. Yang, "All-Optical Format Conversion for Star-8QAM Signals Based on Nonlinear Effects in Elastic Optical Networks," in Journal of Lightwave Technology, vol. 41, no. 2, pp. 440-450, Jan.15, 2023.

[14] Q. Li et al., "Flexible All-Optical 8QAM Signal Format Conversion Using Pump Assisted Nonlinear Optical Loop Mirror," in Journal of Lightwave Technology, vol. 41, no. 20, pp. 6446-6456, Oct.15, 2023.

[15] M. Nölle, F. Frey, R. Elschner, C. Schmidt-Langhorst, A. Napoli, and C. Schubert, "Performance Comparison of Different 8QAM Constellations for the Use in Flexible Optical Networks," in Optical Fiber Communication Conference. San Francisco, CA, 2014, paper W3B.2.

[16] L. Nadal, J. M. Fbrega, J. Vĺlchez, and M. Svaluto Moreolo, "Experimental Analysis of 8-QAM Constellations for Adaptive Optical OFDM Systems," IEEE Photonics Technology Letters, vol. 28, no. 4, pp. 445- 448, 2016.

[17] P. Zou, Y. Liu, F. Wang, and N. Chi, "Mitigating Nonlinearity Characteristics of Gray-Coding Square 8QAM in Underwater VLC system," in Asia Communications and Photonics Conference (ACP), Hangzhou, China, 2018, paper Su4D.3.

[18] P. Song, Z. Hu, and C.-K. Chan, "Performance Comparison of Different 8-QAM Constellations Used in SEFDM systems," in 2021 Opto-Electronics and Communications Conference (OECC), 2021, pp. 1-3.

[19] Q. Wang, Z. Quan, S. Bi, C. Yu, and P.-Y. Kam, "Generalized Mutual Information Analysis for BICM-8QAM With Residual Phase Noise," IEEE Communications Letters, vol. 25, no. 12, pp. 3819-3823, 2021.

[20] Y. Wan, B. Liu, J. Ren, R. Ullah, Y. Mao, S. Zhu, S. Chen, X. Wu, F. Wang, T. Sun, Y. Wu, and L. Zhao, "Performance Enhanced Optical Non-Orthogonal Multiple Access Enabled by Orthogonal Chirp Division Multiplexing," J. Lightwave Technol., vol. 40, no. 16, pp. 5440-5449, 2022.

[21] X. Pan, Y. Liu, and L. Guo, "Asymmetric constellation transmission for a coherent free-space optical system with spatial diversity," Opt. Lett. 46, 5157-5160 (2021).

[22] Hiroki Kishikawa, Masaki Uetai, and Nobuo Goto, "All-Optical Modulation Format Conversion Between OOK, QPSK, and 8QAM," J. Lightwave Technol. 37, 3925-3931 (2019).

[23] Li Q., Yang X., Xu Q., Yang J., Li Y., Yang H, "All-optical aggregation and de-aggregation between OOK, QPSK and 8QAM signals based on

nonlinear effects," Opt. Fiber Technol., Mater. Devices Syst., vol. 77, pp. 103279, May 2023.

[24] Z. Zhong, H. Wang and Y. Ji, "All-optical aggregation and de-aggregation between 3 BPSK and 8QAM in hnlf with wavelength preserved", Appl. Opt., vol. 59, no. 4, pp. 1092-1098, Feb. 2020.

[25] Q. Li, X. Yang, and J. Yang, "All-Optical Aggregation and De-Aggregation Between 8QAM and BPSK Signal Based on Nonlinear Effects in HNLF," J. Lightwave Technol., vol. 39, no. 17, pp. 5432-5438, 2021.

[26] H. Zhang, P.-Y. Kam, and C. Yu, "Performance analysis of coherent optical 8-star QAM systems using decision aided maximum likelihood phase estimation," Opt. Express, vol. 20, no. 8, pp. 9302-9311, 2012.

[27] N. Iiyama, J. ichi Kani, J. Terada, and N. Yoshimoto, "Feasibility Study on a Scheme for Coexistence of DSP-Based PON and 10-Gbps/λ PON Using Hierarchical Star QAM Format," J. Lightwave Technol., vol. 31, no. 18, pp. 3085-3092, 2013.

[28] X. Gong, Q. Zhang, X. Zhang, R. Xuan and L. Guo, "Security Issues and Possible Solutions of Future-Oriented Optical Access Networks for 5G and Beyond," in IEEE Communications Magazine, vol. 59, no. 6, pp. 112-118, June 2021.

[29] Agarwal, R., Bhatia, R. All-optical modulation format conversion between 16-PSK and 8-PSK in elastic optical network. Opt Quant Electron 55, 160 (2023).

[30] Q. Li et al., "Pump-Free and Reconfigurable All-Optical Modulation Format Conversion for MQAM Signals by Parallel Nonlinear Mach-Zehnder Interferometers," in Journal of Lightwave Technology, vol. 42, no. 2, pp. 649-658, Jan. 15, 2024.

[31] S.-B. Cho and T.-G. Noh, "Stabilization of a long-armed fiber-optic single-photon interferometer," Opt. Express, vol. 17, no. 21, pp. 19 027-19 032, Oct. 2009.

[32] G. B. Xavier and J. P. von der Weid, "Stable single-photon interference in a 1-km fiber-optic Mach-Zehnder interferometer with continuous phase adjustment," Opt. Lett., vol. 36, no. 10, pp. 1764-1766, May 2011.

[33] F. Wen, B.-J. Wu, K. Qiu, T. Luo, and Z. Li, "A new feedback control method to stabilize fiber-optical parametric oscillators for clock extraction," Optical Fiber Technology, vol. 19, p. 1C3, Jan. 2013.

[34] Vojtěch Švarc, Martina Nováková, Glib Mazin, and Miroslav Ježek, "Fully tunable and switchable coupler for photonic routing in quantum detection and modulation," Opt. Lett. 44, 5844-5847 (2019).

[35] B. Ham, "Experimental demonstrations of unconditional security in a purely classical regime," Scientific Reports, vol. 11, no. 4149, Feb. 2021.

[36] A. Fallahpour, F. Alishahi, K. Zou, Y. Cao, A. Almaiman, A. Kordts, M. Karpov, M. H. P. Pfeiffer, K. Manukyan, H. Zhou, P. Liao, C. Liu, M. Tur, T. J. Kippenberg, and A. E. Willner, "Demonstration of Tunable Optical Aggregation of QPSK to 16-QAM Over Optically Generated Nyquist Pulse Trains Using Nonlinear Wave Mixing and a Kerr Frequency Comb," J. Lightwave Technol., vol. 38, no. 2, pp. 359-365, 2020.

[37] Arijit Misra, Stefan Preußler, Karanveer Singh, Janosch Meier, Thomas Schneider; Optical channel aggregation based on modulation format conversion by coherent spectral superposition with electro-optic modulators. APL Photonics 1 August 2023; 8 (8): 086112.

[38] J. Prat, J. C. Velsquez and J. Tabares, "Direct PSK-ASK modulation for coherent udWDM", Proc. IEEE 21st Int. Conf. Transparent Opt. Netw., pp. 1-4, 2019.

[39] M. Secondini and E. Forestieri, "Direct Detection of Bipolar Pulse Amplitude Modulation," in Journal of Lightwave Technology, vol. 38, no. 21, pp. 5981-5990, Nov. 1, 2020.

[40] H. Xin, X. Zhang, D. Kong, S. Jia, W. Hu, and H. Hu, "Carrier-recovery-free KK detection for PDM-bipolar-PAM in 100 Gb/s simplified coherent PON," in Optical Fiber Communication Conference (OFC) 2021, P. Dong, J. Kani, C. Xie, R. Casellas, C. Cole, and M. Li, eds., OSA Technical Digest (Optica Publishing Group, 2021), paper F2H.4.

[41] Q. Li and P. Zhu, "All-Optical De-aggregation of 4-Level APSK to 2×BPSK Signals Based on SPM and XPM using HNLF," in Asia Communications and Photonics Conference (ACPC) 2019, OSA Technical Digest (Optica Publishing Group, 2019), paper M4A.57.

[42] H. Wang, L. Pan and Y. Ji, "All-Optical Aggregation and De-Aggregation of 4×BPSK-16QAM Using Nonlinear Wave Mixing for Flexible Optical Network," in IEEE Journal of Selected Topics in Quantum Electronics, vol. 27, no. 2, pp. 1-8, 2021.

[43] H. Kishikawa and N. Goto, "Wavelength Preserved Modulation Format Conversion from 16QAM to QPSK using FWM and SPM," in 2017 Conference on Lasers and Electro-Optics Pacific Rim, (Optica Publishing Group, 2017), paper s0962.

[44] Xiaoxue Gong, Jintao Zhong, Qihan Zhang, Rui Li, and Lei Guo, "Reconfigurable all-optical format conversion for 16QAM/8QAM by employing PSA in HNLF," Opt. Express 31, 22802-22816 (2023).

[45] Qiankun Li, Huashun Wen, Jiali Yang, Qi Xu, Xiongwei Yang and Yameng Li, "All-Optical Regeneration and Format Conversion for 4APSK Signals Based on Nonlinear Effects in HNLF," IEEE Photonics Journal, vol. 15, no. 1, pp. 1-9, Feb. 2023.

[46] J. Yu and X. Zhou, "Ultra-High-Capacity DWDM transmission system for 100G and beyond," in IEEE Communications Magazine, vol. 48, no. 3, pp. S56-S64, March 2010.

[47] M. Kong et al., "640-Gbps/Carrier WDM Transmission over 6,400 km Based on PS-16QAM at 106 Gbaud Employing Advanced DSP," in Journal of Lightwave Technology, vol. 39, no. 1, pp. 55-63, Jan.1, 2021.

[48] Y. R. Zhou, J. Keens and W. Wakim, "High Capacity Innovations Enabling Scalable Optical Transmission Networks," in Journal of Lightwave Technology, vol. 41, no. 3, pp. 957-967, Feb.1, 2023.

[49] Bogris A. "All-optical demultiplexing of 16-QAM signals into QPSK tributaries using four-level optical phase quantizers," Opt. Lett., 39 (7) (2014), pp. 1775-1778.

[50] A. Fallahpour, M. Ziyadi, A. Mohajerin-Ariaei, Y. Cao, A. Almaiman, F. Alishahi, C. Bao, P. Liao, B. Shamee, L. Paraschis, M. Tur, C. Langrock, M. M. Fejer, J. Touch, and A. E. Willner, "Experimental Demonstration of Tunable Optical De-aggregation of Each of Multiple Wavelength 16-QAM Channels into Two 4-PAM Channels," in Optical Fiber Communication Conference, OSA Technical Digest (online) (Optica Publishing Group, 2017), paper Th4I.6.

[51] Francesca Parmigiani, Liam Jones, Joseph Kakande, Periklis Petropoulos, and David J. Richardson, "Modulation format conversion employing coherent optical superposition," Opt. Express 20, B322-B330 (2012).

[52] F. Fresi et al., "Integrated Reconfigurable Coherent Transmitter Driven by Binary Signals," in IEEE Journal of Selected Topics in Quantum Electronics, vol. 21, no. 6, pp. 755-764, 2015.

[53] M. Iqbal, M. Ruiz, N. Costa, A. Napoli, J. Pedro, L. Velasco, Dynamic and efficient point-to-point and point-to-multipoint communications by slicing the optical constellation, in Optical Fiber Communication Conference, Optica Publishing Group, 2022, pp. Th2A-22.

[54] Yu Ding, Hongxiang Wang and Yuefeng Ji, "High-speed all-optical constellation add-drop multiplexer for 16-QAM based on constellation update in elastic optical networks," Optics and Laser Technology, vol. 169, pp. 110028, February 2024.

[55] A. Fallahpour, et al., "Demonstration of 30Gbit/s QPSK-to-PAM4 Data-Format and Wavelength Conversion to Enable All-Optical Gateway from Long-haul to Datacenter," in Optical Fiber Communication Conference, Optica Publishing Group, 2018, paper W2A.22.